

New Joint Design for Three-dimensional Hyper Redundant Robots

Elie Shamma Alon Wolf H. Ben Brown, Jr. Howie Choset
Carnegie Mellon University, Pittsburgh, PA 15213, USA.

eshammas@andrew.cmu.edu, alon.wolf@cmu.edu, hbb@cs.cmu.edu, choset@cmu.edu

Abstract—This paper presents a novel compact design for a two degrees of freedom (DOF) joint mechanism. The joint is optimized for compactness, strength and range of motion which makes it ideal for constructing spatial or three-dimensional hyper redundant robots. We also identify and classify various prior joint designs that led to the development of this new concept. Finally, we present the joint forward kinematics, and force and torque calculations to verify the joint’s range of motion and mechanical advantage.

I. INTRODUCTION

The first serpentine robot was built by Hirose at the Tokyo Institute of Technology (Figure 1a). In his work, he studied how such mechanisms locomote in the plane [6]. The term *hyper-redundant robots* was introduced by Chirikjian and Burdick [1] to describe robots with numerous independent DOF. In their work the authors built a planar device and introduced a variety of methods to solve the inverse kinematic problem for such robots. The work in this paper discusses the mechanical design aspect of joints that are suitable for constructing spatial hyper redundant (SHR) robots, i.e., SHR robots with three-dimensional workspaces. Designing such joints requires balancing many opposing design factors. Particularly, these joints are required to be strong enough to resist high loads generated by the robot’s own weight and other dynamic loads generated by its spatial motions. Nonetheless, the joint should not compromise compactness and maneuverability.

In Section II, we present and discuss four different design approaches used for constructing SHR robots. We also introduce our novel design approach. In Section III we study the forward kinematics of our design and demonstrate the two degrees of freedom: in-plane bending and orienting. We also present the force and torque analysis of our joint to measure its mechanical advantage.

II. MECHANICAL DESIGN OVERVIEW

Researchers have built SHR robots using different approaches. The simplest design consists of connecting several revolute joints together [6], [11]. Another design approach uses a parallel mechanism structure to connect several links together [1] [2] [3]. The need for even more compactness and strength led to angular swivel joints [7], [8]. Finally, we developed a novel joint design which iterates on the angular swivel design and improves on its shortcomings such as strength and range of motion [5].

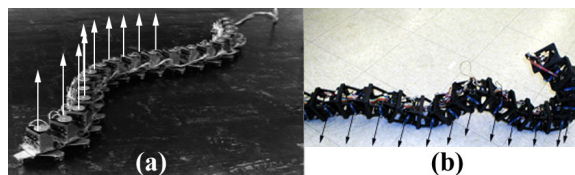


Fig. 1. (a) Hirose’s ACM III snake doing lateral undulation. (b) Our modification of Mark Yim’s PolyBot design, developed at the Sensor Based Planning lab, doing rectilinear locomotion.

A. Actuated revolute joints

Actuated revolute joints provide the simplest design approach to build a snake-like robot. This is done by connecting a sequence of actuated revolute joints in a serial kinematic chain. Many two-dimensional snake robots fall into this category where all the rotation axes of the revolute joints are parallel to each other [11]. Planar snake robots can perform two modes of locomotion: lateral undulation and rectilinear or tracked locomotion. While performing lateral undulation, the snake robot propagates an “S” shaped wave along its body. In this case the revolute joint rotation axes are perpendicular to the ground plane as seen (Figure 1a). In the case of rectilinear or tracked locomotion, these axes are parallel to the ground plane (Figure 1b).

Three dimensional version of this design resembles the two-dimensional design with the exception that the axes of the revolute joints are not parallel. Rather, the rotation axes are skewed to allow motions out of the plane (Figure 2a).

A more compact design is the actuated universal joint where two perpendicular axes coincide at each joint (Figure 2b). The main challenge in this design approach is packaging the actuators within a minimum volume. The actuated revolute joint mechanism has no mechanical advantage, i.e., the motors must react all the external forces applied to the joint. Designers refrain from using direct drive actuators because this approach renders the joint either bulky and strong or small and weak. Using small actuators is only suitable for two-dimensional snake robot since the required reaction forces are relatively small.

To produce strong yet compact SHR robots using revolute joints, designers use high reduction actuators such as power screws or worm gears which tend to slow the joint’s motion. Just recently, Carnegie Mellon’s Sensor

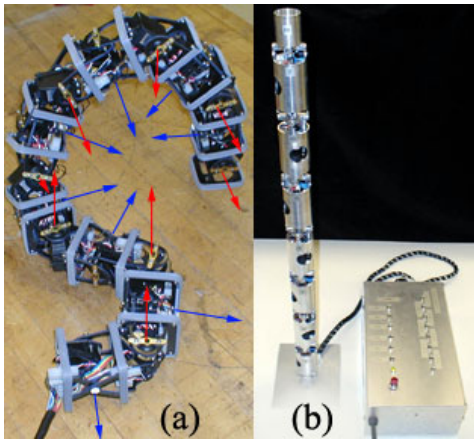


Fig. 2. (a) Our modification of Mark Yim's design used to construct a SHR robot. (b) The actuated universal joint snake robot designed at our lab.

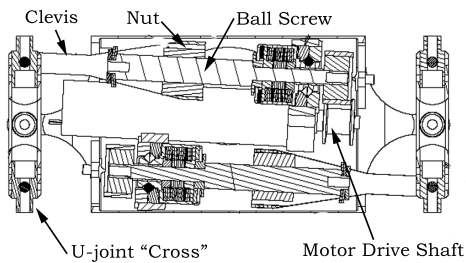


Fig. 3. Detailed view of an actuated universal joint.

Based Planning lab [12] built a snake robot using this design approach (Figure 2b).

In this design, each motor actuates a power screw that drives a nut that is rigidly attached to a clevis which in turn rotates the cross of the universal joint (Figure 3). Each motor actuates one rotation axis of the cross which constitutes one degree of freedom. Two actuators are enclosed inside each link, hence providing two DOF per link. This particular SHR robot has 14 DOF. Each link is 41.7mm in diameter, 96mm in link length and has a ± 55 degrees range of motion. This compact design does not compromise strength and speed. Each joint produces 4.5Nm torque which is enough to cantilever 6 joints. Moreover, each joints takes 5 seconds to travel the entire range of motion.

B. Parallel structure joints

Another design approach used to build snake-like robots uses parallel mechanisms to connect adjacent links. For planar snake robots, a simple closed chain mechanism consisting of linear actuators can constitute the joint connecting two adjacent links or platforms (Figure 4a). For three-dimensional version of this robot, adjacent links are connected together by a non-planar parallel structure.

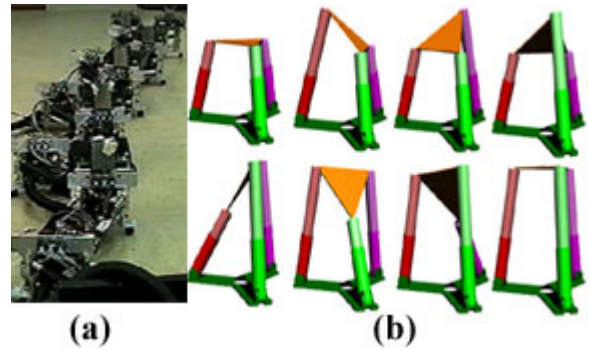


Fig. 4. (a) Planar snake-like robot developed at Caltech using a parallel mechanism. (b) A graphic depicting all configurations of the parallel mechanism using binary actuators.

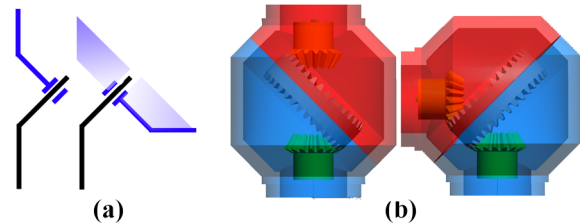


Fig. 5. (a) Supplementary angular shafts. (b) Obliquely cut cups.

The advantages of this design are rigidity, accuracy and strength. However, joints built using parallel mechanism tend to be bulky due to the use of multiple actuators stacked next to each other. Additionally, the joints have a limited workspace. Chirikjian and Burdick have built a planar snake robots using parallel structures [4]. Inspired by Chirikjian work with binary actuators, recently we have been investigating this design approach to build a miniature snake robot using binary actuators. This will reduce the size and the weight of the joint without compromising strength and rigidity (Figure 4b).

C. Angular swivel joints

Angular swivel joints were introduced by Takanashi [7]. The basic idea of this design is to use two angular shafts (Figure 5a), or two obliquely cut cups (Figure 5b), with supplementary angles (the shaft angles sum to 180 degrees). These two shafts are connected by a bearing, hence, rotating one shaft around the other sweeps a cone of revolution. Rotating the other shaft orients this cone of revolution. By coordinating both rotations, the joint can perform two pure motions: in-plane bending (the joint bends in one plane) and orienting (the joint orients the bending plane).

This specific joint design connects two adjacent links of the snake robot via two mechanical paths; hence, the joint has a parallel kinematic structure. The first is through a passive universal joint (Figure 6a), pulling the two

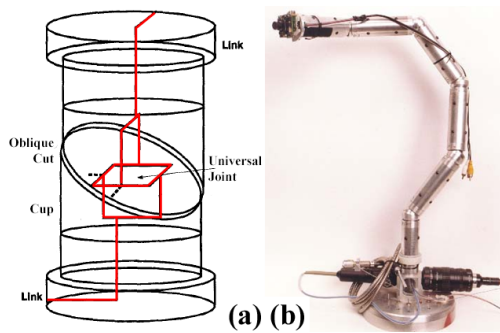


Fig. 6. (a) Angular swivel joint design. (b) JPL snake robot.

links together and the other path is via two obliquely cut spherical cups pushing the two links apart [5]. Even though the joint has only two mechanical paths, the positioning (being concentric) and the form (one being a u-joint and the other having an oblique cut) of the two paths render the joint spatial.

Each cup can be rotated independently using two motors. Rotating both cups in opposite directions yields an in-plane bending motion of the joint. Rotating both cups in the same direction yields an orienting motion of this bending plane. Hence, the two degrees of freedom are coupled since both motors rotate simultaneously at all times. The universal joint prevents twisting between adjacent links; this is extremely crucial for passing signal and power wires inside the robot. However, the universal joint limits the range of motion.

The Jet Propulsion Laboratory (JPL) iterated on Takanashi's design and developed a SHR robot [8] seen in Figure 6b. This snake robot has 14 DOF. Each link is 38.1mm in diameter, 145mm in link length and has ± 60 degrees range of motion. This design has a singularity configuration when the joint is in straight position. In this configuration any motor rotation will lead to bending in one direction, i.e., the orientating DOF is lost. However, this same singularity provides the joint with big mechanical advantage along a direction perpendicular to the bending plane. In other words, the motors do not have to provide any torque to resist external loads in this direction. Moreover, in this particular design the universal joint was put inside the cups. This forced the u-joint to be small which in turn rendered the entire joint relatively weak.

D. Angular bevel joints

Here we introduce our contributions to joint design. This design is similar to the angular swivel joint described above, but it improves on some of its shortcomings. The main difference between the two is the replacement of the universal joint with an angular bevel gear train (Figure 9a). This replacement not only increases the joint's strength but

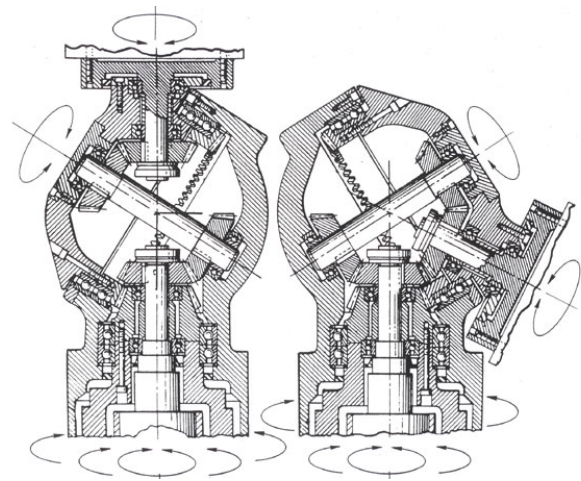


Fig. 7. A section view of a robotic wrist that uses angular bevel gears[10].

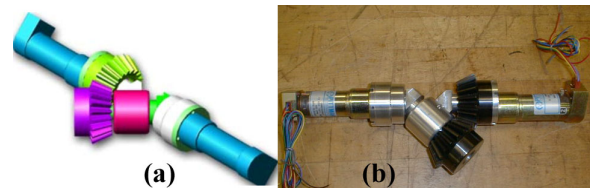


Fig. 8. (a) A 3D model of the joint design. (b) Actual pre-prototype designed and built in our lab as a proof of concept.

also improves its range of motion, which was restricted by the passive universal joint. One of the drawbacks of this design is its mechanical complexity due to the alignment of bevel gears. It is worth mentioning that any industrial robotic arms use designs similar to our proposed design (Figure 7).

So far, we have designed three joints using this approach. Moreover, two working prototypes have been built: the first prototype serves as a proof of concept and was manufactured in the Carnegie Mellon Mechanical Engineering machine shop with standard off-the-shelf parts (Figure 8). This particular prototype has a ± 90 degrees range of motion. Another joint designed using the same approach (Figure 9) is 40mm in diameter, 165mm in length and has ± 90 degrees range of motion. This joint design is patent pending. The latest joint designed is shown in Figure 10. This joint is 40mm in diameter and 170mm in length. It has ± 120 degrees range of motion. All these designs being variants of the angular swivel joint described above have the same singularity configuration that does not allow the joint to move in certain directions instantaneously.

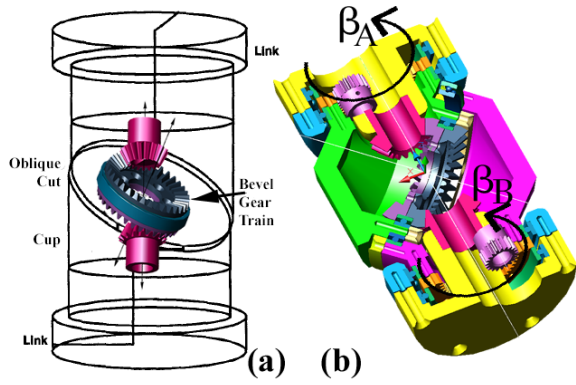


Fig. 9. (a) Bevel gear train replacing the universal joint. (b) Our patent pending joint design.

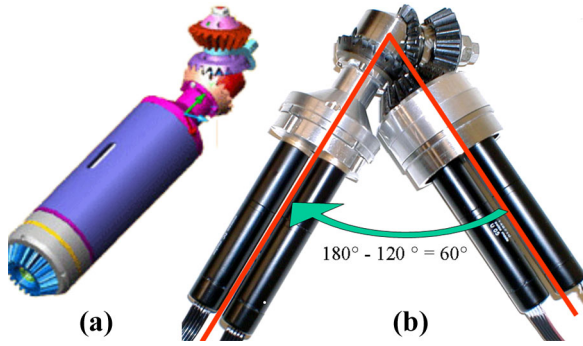


Fig. 10. (a) 3D model of the our latest joint design. (b) Actual prototype of the joint.

III. JOINT ANALYSIS

Here we present an analysis of our novel design (Figure 9b). We also present the force and torque analysis to calculate its mechanical advantage.

A. Forward kinematics of the joint

In order to study the kinematics of the joint, we will find the transformation matrix, \mathbf{T} , that relates motor angles, β_A and β_B , to the actual joint configuration i.e., the two angles: azimuth α and pitch ϕ . We will utilize the fact that the joint is symmetric about the cut plane to simplify our calculations. First we find the transformation matrix \mathbf{T}_A from the motor plate coordinate frame, XYZ_0 , to the obliquely cut face frame, XYZ_3 (Figure 11). Then we multiply these matrices to get the complete solution. The matrix \mathbf{T}_A consists of three rotations: first rotate around Z_0 axis by an angle β_A (\mathbf{T}_0^1), then rotate around the new Y_1 axis by 45 degrees (\mathbf{T}_1^2) and lastly by rotate around the new Z_2 axis by an angle $\beta_A/2$ (\mathbf{T}_2^3). Multiplying these matrix transformations we get: $\mathbf{T}_A = \mathbf{T}_2^3 \cdot \mathbf{T}_1^2 \cdot \mathbf{T}_0^1$.

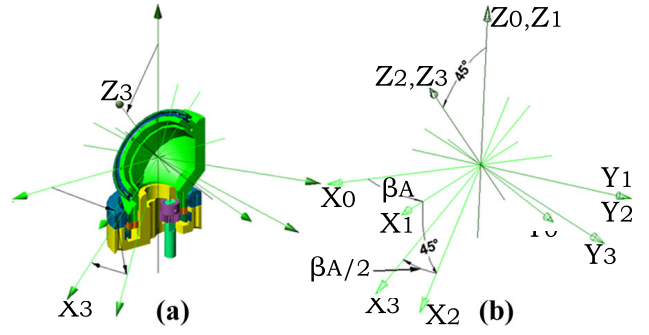


Fig. 11. Coordinate frames used to calculate the matrix transformation \mathbf{T}_A .

$$\mathbf{T}_A = \begin{bmatrix} \frac{C_{\beta_A}^2}{\sqrt{2}} + S_{\beta_A}^2 & \frac{C_{\beta_A} S_{\beta_A}}{\sqrt{2}} - S_{\beta_A} C_{\beta_A} & -\frac{C_{\beta_A}}{\sqrt{2}} \\ \frac{S_{\beta_A} C_{\beta_A}}{\sqrt{2}} - C_{\beta_A} S_{\beta_A} & \frac{S_{\beta_A}^2}{\sqrt{2}} + C_{\beta_A}^2 & -\frac{S_{\beta_A}}{\sqrt{2}} \\ \frac{C_{\beta_A}}{\sqrt{2}} & \frac{S_{\beta_A}}{\sqrt{2}} & \frac{1}{\sqrt{2}} \end{bmatrix} \quad (1)$$

where C_{β_A} and S_{β_A} stand for $\cos(\beta_A)$ and $\sin(\beta_A)$ respectively. Doing the same calculation for the second half of the joint we compute $\mathbf{T}_B = \mathbf{T}_6^7 \cdot \mathbf{T}_5^6 \cdot \mathbf{T}_4^5$. Finally we compute the total transformation matrix, we get

$$\mathbf{T}(\beta_A, \beta_B) = \quad (2)$$

$$\begin{bmatrix} \frac{1}{2} [C_{\beta_A}^2 C_{\beta_B} + \sqrt{2} C_{\beta_B} S_{\beta_A}^2 + C_{\beta_A} (-1 + (-1 + \sqrt{2}) S_{\beta_A} S_{\beta_B})] \\ \frac{1}{2} [-S_{\beta_A}^2 S_{\beta_B} - \sqrt{2} S_{\beta_B} C_{\beta_A}^2 - S_{\beta_A} (-1 - (-1 + \sqrt{2}) C_{\beta_A} C_{\beta_B})] \\ \cos^2(\frac{\beta_A + \beta_B}{2}) \end{bmatrix}$$

Starting from a straight position, we represent the next bay by the vector $V = (0, 0, 1)$, the axis of the next link is along the Z axis of the XYZ_7 coordinate frame. After a specified angular rotation of each motor, the vector V will be transformed to a new vector $V' = (V_x, V_y, V_z)$ which specifies the new orientation of the next bay axis, the new Z axis after rotating frame XYZ_7 . This is done by multiplying vector $V = (0, 0, 1)$ by the transformation matrix given in equation (2).

The joint was designed so that the motors run at the same speed, hence, we set $|\beta_A| = |\beta_B| = \beta$. Finally we compute the final configuration of the joint:

$$\mathbf{V}'^+(\beta, \beta) = \begin{bmatrix} \mathbf{V}'_x \\ \mathbf{V}'_y \\ \mathbf{V}'_z \end{bmatrix} = \begin{bmatrix} (1 - \sqrt{2}) C_{\beta} S_{\beta}^2 \\ -\frac{1}{2} (1 + \sqrt{2} + (-1 + \sqrt{2}) C_{2\beta}) S_{\beta} \\ C_{\beta}^2 \end{bmatrix} \quad (3)$$

$$\mathbf{V}'^-(\beta, -\beta) = \begin{bmatrix} (1 - \sqrt{2}) C_{\beta} S_{\beta}^2 \\ \frac{1}{2} (1 + \sqrt{2} + (-1 + \sqrt{2}) C_{2\beta}) S_{\beta} \\ C_{\beta}^2 \end{bmatrix} = \begin{bmatrix} \mathbf{V}'_x \\ -\mathbf{V}'_y \\ \mathbf{V}'_z \end{bmatrix} \quad (4)$$

$$\mathbf{V}'^-(\beta, -\beta) = \mathbf{V}'^-(\beta, \beta) = \begin{bmatrix} 0 \\ 0 \\ 1 \end{bmatrix} \quad (5)$$

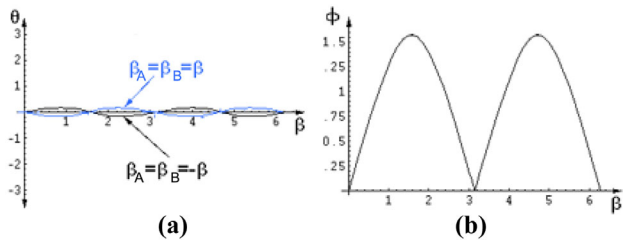


Fig. 12. Azimuth and pitch angles versus motor angle for bending mode of motion.

V'^+ and V'^- represent the new joint configuration when the motors are turning in the same or opposite directions respectively. Equation (3) displays the bending motion starting from the straight configuration. Equation (5) verifies the orientation motion. Since we start in a straight configuration the orientation DOF does not move the joint at all but both cups rotate as one rigid body. Finally, we compute the pitch and azimuth angles, ϕ and θ , for the bending mode of motion:

$$\phi = \cos^{-1}\left(\frac{V'_z}{\|V'\|}\right) = \cos^{-1}(\cos^2(\beta)) \quad (6)$$

$$\theta = \tan^{-1}\left(\frac{V'_y}{V'_x}\right) = \tan^{-1}\left(\frac{((-1 + \sqrt{2})\cos(2\beta) + \sqrt{2} + 1)\csc(\beta)\sec(\beta)}{2(-1 + \sqrt{2})}\right) \quad (7)$$

Plotting these angles versus motor the angle verifies that bending occurs almost in a plane. The joint's maximum bending angle is 90 degrees (Figure 12).

B. Force and torque analysis

Now we study how external joint loads are transferred to the motors. To do so, we study the worst case configuration scenarios that generate the maximum loads at the base joint of a SHR robot under its own weight. Assuming a SHR robot comprises n links, where each link has length L and weight W . We identify two worst case scenarios: **Case 1**: the snake robot is fully extended horizontally and the base joint has to cantilever the rest of the body of the snake (Figure 13a). In this case the base joint experiences the highest shearing and bending moment loads. **Case 2**: the snake is in an "L" shape configuration where the base joint is loaded with the highest twisting torque (Figure 13b).

Now we study how the external loads T_x and T_y are transferred through the joint structure to the motors. As an intermediate step we calculate the loads on the bevel gear, T_g , and the obliquely cut face, T_f . Then we compute the motor torque, T_{MOTOR} , required to resist these external loads. Solving for T_g and T_f we get:

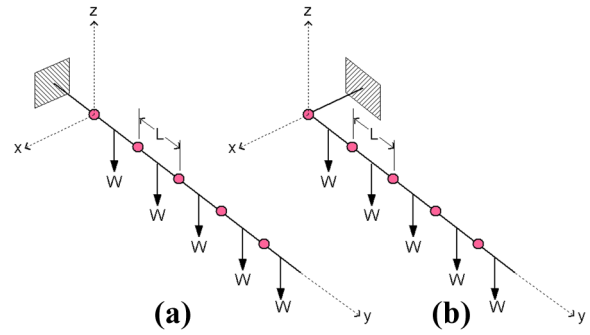


Fig. 13. Case 1 and Case 2 configurations.

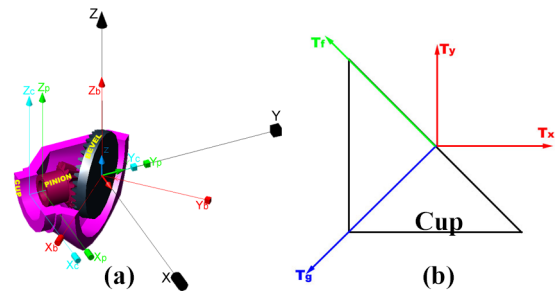


Fig. 14. External loads T_x and T_y are resisted by T_g and T_f .

$$\begin{aligned} \Sigma T_x = 0 &\Rightarrow -T_f \cos \alpha - T_g \sin \alpha + T_x = 0 \\ \Sigma T_y = 0 &\Rightarrow T_f \sin \alpha - T_g \cos \alpha + T_y = 0 \\ T_g &= T_x \sin \alpha + T_y \cos \alpha \\ T_f &= T_x \cos \alpha - T_y \sin \alpha \end{aligned} \quad (8)$$

where $\alpha = \pi/4$ is the cup cut angle. Solving the total motor torque for case one we get:

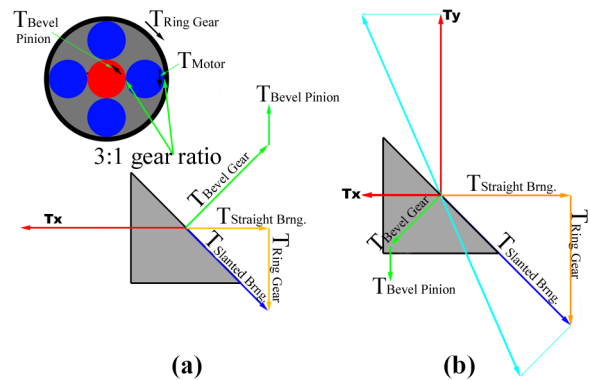


Fig. 15. Free body diagram for the base joint in (a) Case 1. (b) Case 2.

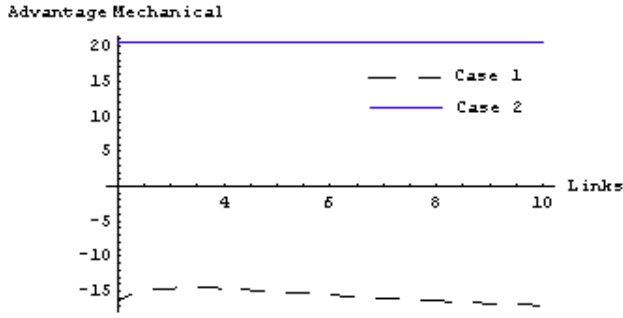


Fig. 16. Mechanical advantage of the joint versus the number of links.

$$T_x = 0, \quad T_y = n^2 \frac{WL}{2}, \quad T_f = \frac{n^2}{\sqrt{2}} \frac{WL}{2}, \quad T_g = \frac{n^2}{\sqrt{2}} \frac{WL}{2}$$

$$T_{Motor} = \frac{1}{3} \left(\frac{T_f}{\sqrt{2}} + \frac{T_g}{2} \right) = \frac{n^2(2+\sqrt{2})}{24} WL \quad (9)$$

Doing the same calculation for case 2 we get:

$$T_x = (2n-1) \frac{WL}{2}, \quad T_y = (n-1)^2 \frac{WL}{2}$$

$$T_f = \frac{n^2}{\sqrt{2}} \frac{WL}{2}, \quad T_g = \frac{n^2 - 4n + 2}{\sqrt{2}} \frac{WL}{2}$$

$$T_{Motor} = \frac{1}{3} \left(\frac{T_f}{\sqrt{2}} - \frac{T_g}{2} \right) = \frac{2n^2 - \sqrt{2}(2-4n+n^2)}{24} WL \quad (10)$$

Figure 16 gives the plot of the ratio of external load torques, T_x and T_y , to motor torques of the joint versus the number of links for each of the two cases. Even in these worst case scenarios, the ratio stays above 15 in **case 1** and a constant 20 in **case 2**. The reason for the *high* ratio is due to the gear reduction inherent in the joint design, allowing us to use even smaller motors to actuate the joint.

IV. CONCLUSION

Joint mechanism design has been a bottleneck for constructing compact, strong and maneuverable SHR robots. Moreover, a multitude of new robotic applications such as search and rescue, jet engine inspection, low profile locomotion, etc., have highlighted the need for such robots. In this paper we have presented a promising novel joint mechanism design that optimizes strength and compactness while maintaining high dexterity.

We have designed three joints variants of the same concept so far and manufactured two prototypes that have served to verify our claims. The results are promising and we will soon build a complete SHR robot using this novel joint design. In the future we look forward to design SHR robots using alternative actuators. Polymer muscles are a promising form of actuation but the technology is still in the developing stages [9].

ACKNOWLEDGEMENT

The authors would like to thank Eric Rollins, Shigeo Hirose, Nobuaki Takanashi and Jonathan Luntz for their valuable input to our work. We would also like to thank members of both university machine shops for their great work and cooperation: James Schubert, Steve Hoffman, Dave Belotti, Jim Dillinger and John Fulmer.

V. REFERENCES

- [1] G.S. Chirikjian and J. Burdick. Kinematics of hyper-redundant locomotion with applications to grasping. In *Proc. IEEE Int. Conf. on Robotics and Automation*, pages 720-727, Sacramento, CA April 1991.
- [2] G.S. Chirikjian and J. Burdick. Kinematically optimal hyper-redundant manipulator configurations. In *IEEE Transactions on Robotics and Automation* 11: 794-806, 1995.
- [3] G.S. Chirikjian and J. Burdick. A modal approach to hyper-redundant manipulator kinematics. In *IEEE Transactions on Robotics and Automation* 10: 343-354, 1994.
- [4] G.S. Chirikjian, J. Burdick, A Hyper-Redundant Manipulator, In *IEEE Robotics and Automation*, 1: 22-29, December 1994.
- [5] H. Choset, J. Luntz, E. Shamma, T. Rached, D. Hull and C. Dent. Design and Motion Planning for Serpentine Robots, in *Proc. of the Tokyo Institute of Technology Super Mechano Systems Workshop*, Tokyo, Japan, 2000.
- [6] S. Hirose. "Biologically Inspired Robots: Snake-Like Locomotors and Manipulators," Oxford University Press, 1993.
- [7] H. Ikeda and N. Takanashi. *Joint Assembly Movable Like A Human Arm*, U. S. Patent 4 683 406, July 1987.
- [8] E. Paljug, T. Ohm and S. Hayati. The JPL Serpentine Robot: a 12-DOF system for inspection, in *Proc. of the 1995 IEEE/ICRA*, Volume: 3, 1995 Page(s): 3143-3148
- [9] R. Pelrine, R. Kornbluh, J. Eckerle, P. Jeuck, S. Oh, Q. Pei, and S. Stanford. 2001. Dielectric Elastomers: Generator Mode Fundamentals and Applications, in *Proc. SPIE Electroactive Polymer Actuators and Devices*, ed. Y. Bar-Cohen, Vol. 4329, Newport Beach, California (March).
- [10] M. E. Rosheim. *Robot Wrist Actuators*. John Wiley and Sons (February 1989)
- [11] M. Yim. "Locomotion with a Unit Modular Reconfigurable Robot," PhD Thesis, Dept. of Mech. Eng. Stanford Univ. 1994
- [12] A. Wolf, H.B. Brown, R. Casciola, A. Costa, M. Schwerin, E. Shamma and H. Choset. A Mobile Hyper Redundant Mechanism for Search and Rescue Tasks. To be published in IROS 2003.